JOURNAL OF PROPULSION AND POWER
Vol. 23, No. 5, September–October 2007

Passive Control of Forced Combustion Instability in a Swirl-Stabilized Spray Combustor

M. Linck* and A. K. Gupta†
University of Maryland, College Park, Maryland 20742

DOI: 10.2514/1.15933

A coannular swirl-stabilized burner, equipped with a pulsation mechanism to introduce controlled periodic instability into the fuel flow to the nozzle, was used to examine instability mechanisms and demonstrate passive control of combustion instability. The effects of swirl configuration and airflow distribution on forced, unstable combustion were examined. Fuel pulsation was used to excite a dynamic response from the combustor that would mimic the behavior of instabilities encountered in many commercial, military, and industrial systems. The response of a spray flame to pulsations of different frequencies was examined using a sound spectrum analyzer and particle image velocimetry. The effect of swirl distribution in the burner, including co- and counterswirl distribution, on the amplitude response of three different flames to low-frequency fuel pulsation was examined. An analysis of the flame structure at different points during the cycle of a forced, low-frequency instability is presented for three swirling spray flames. The effect of airflow distribution on the dynamic response of one flame obtained with a particular swirl configuration is presented. Changes in swirl distribution, which affected recirculation and mixing, were found to reduce the magnitude of the flame response to forcing. Changes in airflow distribution, which affected residence times of product gases in the combustion region, were also found to reduce the combustor response to forcing. Changes in swirl and airflow distribution in a burner of this type were shown to provide effective passive control of combustion instabilities.

Introduction

INSTABILITIES in combustors develop when cyclical heat-release mechanisms in the combustor become coupled to some characteristic frequency of the combustor. Often, this is the Helmholtz frequency of the combustor, although other components of the combustion system, such as the inlet duct or the exhaust duct, may also be important in determining the frequency of the instability [1]. Once unstable combustion develops, both the heat release and the pressure in the combustor will fluctuate periodically. The coupling of the heat-release mechanism with the characteristic frequency of the combustor must meet the Rayleigh criterion [2] in order to drive the instability. The Rayleigh criterion requires that the cyclical heat release must oscillate with a period that is similar to the period of the pressure fluctuation, and is nearly in phase with it. Oscillations may occur on a large range of time scales, but only those corresponding to natural acoustic frequencies of the combustor will be amplified. If the curves are out of phase, the amplitude of the instability is likely to remain small.

The dominant frequency involved in unstable behavior depends on the combustor geometry, and on the resonant frequencies of equipment associated with the combustor. The possible frequencies depend on the local speed of sound in a given component, and each component has multiple acoustic modes [1]. Because acoustic waves can propagate in up to three dimensions in each component, it is difficult to predict which frequency is most likely to be associated with combustor instability in a particular system. Unstable combustion can be readily characterized via the sound spectrum emitted by the combustor. Frequencies represented in the sound spectrum are associated with the turbulent mixing in the flow, and peaks in the spectrum indicate that turbulent events occur at particular frequencies that drive mixing and combustion in the system [3]. The sound spectrum of an unstable combustor is generally dominated by the frequency of the instability, and this frequency will have an associated sound pressure level many orders of magnitude greater than that of the other frequencies in the spectrum [1].

In order for instability to be driven, oscillations in pressure due to acoustic resonance in the combustor must be linked to heat release from the combustor. Usually, the mechanism depends on interaction between the oscillating pressure in the combustor and the evolution and breakdown of turbulent structures involved in combustion. Schadow and Gutmark [4] illustrate this point in a review on the nature and control of flame instabilities. Their analysis of unstable gas-fueled dump combustors describes the role of vortex behavior in the development of instabilities. Vortical structures in the combustor form and break down in a cyclical fashion, which causes mixing between the fuel and the oxidizer, and the associated heat release, to increase and decrease cyclically.

Turbulent events and turbulent structures occur over a wide range of temporal and spatial scales in any turbulent flow and determine the rate of mixing between fuel and oxidizer in a combustor. Because the heat-release rate is affected by the phenomenon of mixing, the dynamic heat release in the combustor is linked to the time scales of turbulent mixing events occurring in the combustor [4]. When the time scale of a particular turbulent event matches the time scale of an acoustic mode in the system, the evolution and breakdown of a particular turbulent structure may become synchronized with the oscillation in pressure in the combustor. The turbulent structure in question depends on the flow. In a burning jet the instability may be linked to the shedding of vortices at the jet boundary [5]. In a dump combustor or bluff-body stabilized combustor, the instability may be linked to oscillations in the size and location of the recirculation region, even though vortices are not shed [1]. The unsteady heat release in the combustor can then drive instabilities, as long as it is sufficiently in phase with a characteristic frequency of the combustor. If the turbulent structures affecting heat release in the flame can synchronize effectively with an acoustic mode, unstable combustion can occur.

The objective of the present investigation is to examine the dynamic response of unconfined swirl-stabilized flames, fueled by

Received 26 April 2005; revision received 29 January 2006; accepted for publication 19 February 2006.

*Ph.D. Student, The Combustion Laboratory, Department of Mechanical Engineering.

†Professor, The Combustion Laboratory, Department of Mechanical Engineering; akgupta@eng.umd.edu.

kerosene, to periodic changes in the equivalence ratio, leading to unstable flame behavior. Controlled, periodic variation of the equivalence ratio is achieved via pulsation of the fuel supplied to the flame. The global flame features associated with each operating condition are examined and are related to features of the recirculation region in the combustion airflow. Specific effects of swirl configuration and airflow distribution on the dynamic response of the flame are discussed, in order to identify flame features and frequencies that are likely to be linked to unstable combustion, and to illustrate practical strategies for passive combustion control.

Passive Control of Instabilities

Because of the role played by large-scale vortical structures in the development of combustor instabilities, considerable work has been done to disrupt the formation of these structures. Instability can be avoided if the turbulent events affecting mixing and heat release in the flow can be altered in such a way that events associated with instability cannot dominate the rate of heat release.

Passive control of combustion instabilities depends on alterations in the combustor that do not actively respond to the onset or amplification of unstable behavior. An example of this type of modification in a dump combustor is described by Schadow et al. [6]. A similar modification of a swirl-stabilized combustor is described by Paschereit and Gutmark [7]. In both cases, the geometry of the combustor was altered to introduce fine-scale turbulence into the flow, ensuring that mixing and heat release occurred on time scales other than those associated with large, vortical structures. In the dump combustor, combustion was stabilized by the installation of a series of small steps, rather than a single large one [6]. In the swirl-stabilized combustor, small vanes were installed at particular points, to change the behavior of the local boundary layer and create small-scale turbulence in certain regions of the flow [7]. Both approaches are examples of passive instability control. Both studies show that the amplitude of the instability was controlled, because the unstable features of the flow could not effectively synchronize with an acoustic mode in the system once the modifications to combustor geometry were made [6,7].

The use of noncircular or modified nozzles has also been examined to strategically control the behavior of large-scale vortical structures in combustors. Gutmark and Grinstein [5] provide a comprehensive review of the work done on noncircular nozzles. The most important observation is that nozzles with varying radii of curvature along their perimeter (such as rectangular nozzles, for example) produce different turbulent flow structures in different regions of the flow. Sides of the nozzle that are straighter, and have large radii of curvature, produce larger vortical structures. Regions where the radius of curvature is small create small, high-frequency vortical structures. This phenomenon is of particular interest, because instabilities in combustors are often linked to the dynamic behavior of large vortical structures, which break down into fine-scale turbulence in a cyclical manner, releasing heat and driving oscillations. Because noncircular nozzles seem to promote both large- and small-scale turbulence, these nozzles can be used to promote mixing on a range of spatial and temporal scales, altering or eliminating unstable combustion [5].

Hu et al. [8] investigated the addition of mechanical tabs that protrude out into the flow at the exit of the nozzle to increase mixing of the flow in jet engines. These tabs were designed to cover approximately 1.5% of the exit area of the nozzle. The mechanical tabs produced small vortices, whose size was dependent on the tab dimensions, at the exit of the nozzle. Small-scale turbulent structures appeared farther upstream in the flow when tabs were present, indicating that the addition of the tabs destabilized the interface between the jet and surrounding fluid, and promoted mixing over an expanded range of turbulent scales [8].

Combustor instability may also be linked to changes in the inlet equivalence ratio. Steele and Cowell [9], working in conjunction with Smith and Cannon [10], present an experimental and analytical approach to stability control that incorporated a dynamically varying inlet equivalence ratio. Heat release is a function of the equivalence ratio in the combustion zone; if the mixture becomes too lean or too rich, the adiabatic flame temperature of combustion decreases. If the equivalence ratio moves toward unity, near stoichiometric combustion, the combustion temperature at the flame front rises [3]. Based on the work of Richards and Janus [11], Steele and Cowell modeled an experimental combustor as a Helmholtz resonator during unstable combustion, and determined the most likely frequency of unstable combustion. They observed that the airflow rate into the combustor will become unsteady when the pressure in the combustion chamber pressure oscillates. If one assumes that the fuel flow rate is unaffected by the combustor pressure oscillations (as is often the case in practical systems, where fuel is delivered at very high pressure [12]), it becomes clear that the equivalence ratio of the air–fuel mixture entering the combustor will also become a function of time, because the proportions of air to fuel will be altered by the oscillatory behavior of the combustion airflow rate. The location of the fuel injector in the mixing plenum can then be adapted so that, when the instability develops, the fuel enters the combustion chamber in a manner that is out of phase with the instability [10,11]. To control the instability, the injector is located so that when the oscillatory pressure nears its peak amplitude in the combustor and the airflow rate drops, the resulting accumulation of fuel does not reach the combustor until the pressure in the combustor has decreased back to the minimum value. If the fuel always arrives at a point in the instability cycle when the combustor pressure is reduced, the instability will be effectively damped [9]. Experimental work confirmed that combustion instability was successfully controlled via this approach [9,10].

A very similar approach is described by Lubarsky and Levy [13]. They show that an effervescent spray injection system can control instability when correctly configured. The liquid-fueled ramjet combustor used in their study incorporated a low-pressure effervescent atomizer. In a standard pressure atomizer, the liquid fuel is converted into a spray when it is forced at high pressure through a small orifice, into a region of much lower pressure [12]. Effervescent atomizers force air bubbles into the fuel in a small mixing chamber upstream of the final orifice. The pressure drop across the orifice is lower than that for pressure atomizers, but the gas bubbles in the fuel stream destabilize the stream, effectively atomizing the fuel. Because an effervescent atomizer operates at a relatively low-pressure drop, the amplitude of the pressure signal from the combustor instability represents a considerable fraction of the total pressure drop across the atomizer. Thus, the amount of fuel atomized can change dramatically in response to the pressure changes in the combustor. If this pulsating component of the total fuel fed to the combustor is sufficiently large, and sufficiently out of phase with the signal from the combustor, the combustion instability in the combustor will be damped [10].

Unstable combustion can be affected by the turbulent features of the flame, the acoustic modes of the combustion system, and changes in the equivalence ratio that become linked with the instability. The present study examines the effect of these parameters on the unstable behavior of a turbulent, swirl-stabilized spray flame.

Swirl stabilization of combustion is a common technique, widely applied in practical combustion systems as described by Gupta et al. [14]. If rotation is imparted to a flow, it can be characterized by a swirl number S, which provides a comparison of rotational momentum and axial momentum. If the swirl number at the inlet to a combustor is greater than a critical number of approximately 0.6, vortex breakdown occurs at the center of the flow, and a toroidal recirculation region is formed, resulting in flow recirculation. Flames are commonly stabilized at the surface of the recirculation region, where fresh fuel and oxidizer mixes with the hot recirculating product gases [14]. Multiple concentric air annuli, each featuring a particular swirl number, can be employed to shape the features of the flow and flame [15]. The resulting flow displays complex turbulent behavior over a wide range of scales, and modeling of flows of this type is difficult [16]. Because of the complexity of the flow, it is also difficult to predict the possible unstable behavior of the flame. However, swirling flows can be manipulated to create desirable flame features. Linck et al. [17] have shown that the interaction

between a fuel spray and the flow can be altered by changes in the swirl conditions and flow features of the combustion air. Linck et al. [18,19] and Gupta and Linck [20] have also shown that the geometry and stability characteristics of the flame can be altered dramatically by changes in the swirl conditions introduced into the flow.

New analytical techniques, which will help to develop an understanding of combustor instabilities, are also being developed. For example, a new particle image velocimetry (PIV) technique, capable of overcoming the challenges inherent in examining the behavior of the flowfields of luminous flames, has recently been introduced [21]. PIV in luminous reacting flows using charge-coupled device (CCD) detectors is problematic, because the second image in an image pair tends to be overexposed. The new method uses narrow bandpass filters and mechanical shutters to ensure consistent illumination of the detector [21]. Linck and Gupta [22] show that the technique can be applied to examine the flowfield of the fuel spray in highly luminous swirl-stabilized kerosene flames.

Passive control of combustion instabilities in swirl-stabilized flames is also described by Conrad et al. [23] using n-heptane as the fuel. The fuel was atomized by tangentially entering combustion air in a primary air duct. The swirling air–fuel mixture, with entrained fuel droplets, exited this primary duct, and was brought into contact with swirling air exiting a secondary air duct. The outer, secondary air swirled in the opposite direction, creating a counterswirl condition. A quartz tube was fitted around the flame and extended downstream. In nonreacting cases, examined without the quartz tube enclosure using a phase-Doppler particle analyzer (PDPA), the investigators showed that one could alter the structure of the spray by changing the amount of air fed through the inner and outer ducts. They also examined the heat-release signature of the enclosed flame using a photomultiplier tube detector tuned to the light emission frequency of the CH radical. They found that the dominant unstable modes associated with the heat-release signal from the flame could be shifted slightly in frequency by changes in the airflow distribution. The amplitude of the peak instability and the fuel spray structure could be affected dramatically by changes in airflow distribution between the primary and secondary ducts [23].

Conrad et al. [23] showed that the flowfield has an effect on the dynamic response of a liquid-fueled spray flame. However, because they used a tangential-entry system to feed combustion air to their flame, the exact swirl distribution at the inlet of their burner was unknown. This situation complicates analysis and modeling considerably. Also, because their configuration examined only the behavior of flames in counterswirling flows, it would be useful to examine the behavior of flames in coswirling flows, where the air from each annulus rotates in the same direction. The flames examined by Conrad et al. displayed instabilities above 400 Hz; however, instabilities at much lower frequencies are often present in practical combustion systems, driven by characteristic frequencies of large components [1]. The introduction of a forcing signal, driving an unstable response from the flame, can help clarify the effect of swirling flow parameters on the dynamic response of the combustor. Conrad et al. investigated a single-component fuel [23]. Real fuels, such as kerosene or Jet-A are composed of large mixtures of compounds, featuring a wide range of properties. Fuel droplets composed of mixtures vaporize differently than do single-component fuels [24,25] and this may affect the dynamic behavior of the flame. Conrad et al. investigated a flame featuring a very fine fuel spray with a Sauter mean diameter of approximately 17 μm [23]. Practical liquid-fueled combustors generally feature fuel sprays with much larger droplet diameters, on the order of 50 μm [12]. Larger droplets are not entrained as readily, and this effect may alter the unstable response of the flame. The current investigation addresses these issues directly.

Experimental Facility and Conditions

To provide good control of the swirl and airflow distribution, a burner featuring two coannular air ducts was equipped with swirl vane assemblies at the outlets. A schematic diagram of the burner used is shown in Fig. 1. The coannular air ducts fed combustion air to

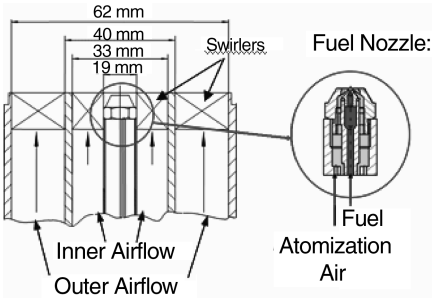

Fig. 1 Schematic diagram of the spray burner and fuel nozzle.

the flame, and an air-assisted atomizing fuel nozzle, located at the centerline, was used to disperse the fuel. The air-assisted nozzle used a high-speed swirling stream of atomizing air to destabilize the fuel jet, creating a fine spray. Nozzles of this type have found wide practical application in combustion systems and provide effective atomization over a wide range of fuel flow rates [12]. Because the swirl characteristics of the flow could be adjusted at will, both co- and counterswirl flames were examined to determine the effect of swirl on the dynamic response of the flame. The dynamic pressure signal from the flame was examined via the sound pressure level (SPL) spectrum of each flame. To excite a large-amplitude unstable response from the combustor, a forcing signal was introduced at frequencies between 10 and 250 Hz. This signal consisted of a periodic interruption of the fuel flow upstream of the fuel nozzle, and hence, a periodically oscillating fuel flow rate and equivalence ratio at the nozzle. The introduction of a forcing mechanism allowed one to examine the flame response to a range of instability frequencies.

The swirl assemblies in the air annuli featured straight swirl vanes. Straight swirl vanes have a vane angle that does not vary with radial location. The swirl number S of a straight-vane swirl assembly can be approximated [14] as

$$S = 2/3\left[\frac{1-(d_h/d_o)^3}{1-(d_h/d_o)^2}\right]\tan(\theta) \tag{1}$$

where d_h is the hub diameter of the swirler, and d_o is the outer diameter of the swirler. Thus the swirl number is found to depend primarily on θ, the swirl vane angle. Swirl vanes featuring angles greater than 70 deg from the burner centerline cannot usually be employed in practice. In this study the inner swirlers featured swirl angles of 30 and 45 deg from the vertical centerline of the burner. The outer swirlers featured swirl angles of 50 and -50 deg. The swirlers used and the respective calculated swirl numbers are shown in Table 1. The sign of the swirl number indicates the swirl sense; positive swirl numbers indicate clockwise rotation (looking into the burner from the top), while negative swirl numbers indicate counterclockwise rotation.

A mean fuel flow rate of 0.5 gal/h was fed through the fuel nozzle. An atomization airflow rate of 0.25 SCFM (standard cubic feet per minute) was necessary to obtain the desired atomization of the fuel. Droplet sizes of approximately 50 μm were observed, and a solid-cone fuel spray, with an included angle of approximately 60 deg was produced. The fuel spray produced by the nozzle was characterized in previous investigations using a 2-D phase-Doppler particle analyzer [17,20]. The PDPA technique is described in detail by Bachalo and Houser [26]. Properties of the fuel spray produced by the nozzle are presented in Fig. 2. Because the fuel spray was affected by the surrounding airflow, the spray was examined under combustor

Table 1 Swirl numbers of swirl vane assemblies

Swirler type	Swirler vane angle	Swirl no.
Inner	30 deg	0.385
Inner	45 deg	0.667
Outer	50 deg	0.795
Outer	−50 deg	−0.795

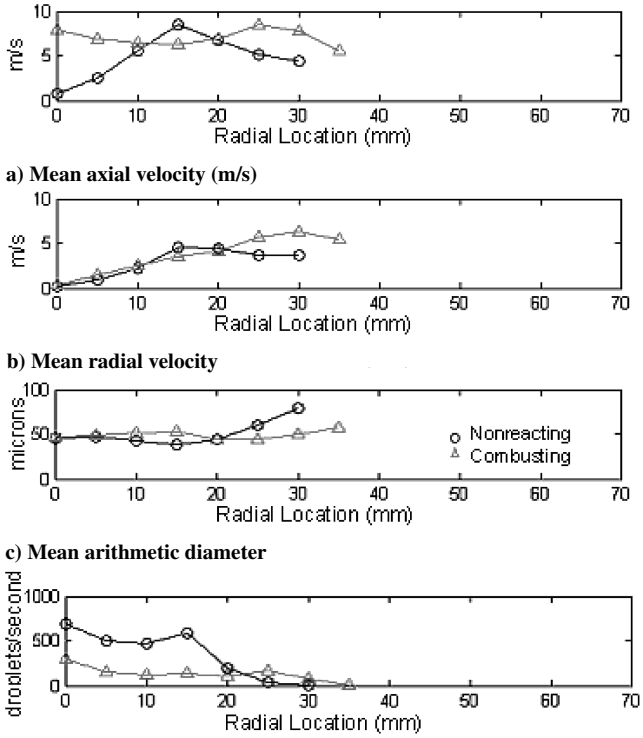

Fig. 2 Fuel spray characteristics from the atomizing nozzle at 30 mm downstream from the atomization nozzle using 30/50 deg combustion air swirl configuration, 50/50% airflow distribution, 28.6 SCFM total airflow rate.

swirl and airflow conditions representative of those employed in the spray flames that form the basis of this investigation. Data shown in Figs. 2a–2d taken at 30 mm downstream of the atomization nozzle exit show mean axial velocity, radial velocity, arithmetic mean diameter, and droplet number density in the spray, respectively, for both a nonreacting and combusting spray. The mean fuel droplet diameter was found to vary with spatial location within the spray, presence or absence of combustion, and the airflow parameters (airflow distribution and swirl configuration). The arithmetic mean diameter of the fuel spray obtained is representative of many fuel sprays in practical systems. Further details on the properties of the spray are given by Linck et al. [17].

Three different swirl configurations were employed here. Their characteristics are listed in Table 2. In the first configuration, the inner annulus swirl vane angle was 45 deg while the outer annulus swirl vane angle was 50 deg (both from the vertical axis of the burner). This is referred to as the 45/50 deg swirl configuration. The second swirl configuration featured an inner swirl angle of 30 deg, and an outer swirl angle of 50 deg. This is referred to as the 30/50 deg configuration. Both the 45/50 deg and 30/50 deg swirl configurations were coswirling, meaning that the air from each duct rotated in the same direction. The third swirl configuration employed a counterswirling configuration, with an inner annulus swirl vane angle of 30 deg and an outer annulus swirl vane angle of −50 deg. This counter-rotating configuration is referred to as the 30/−50 deg configuration. The objective of this counter-rotating swirl configuration was to examine the effect of the high-shear region formed between the inner and the outer annulus airflows where the two counter-rotating flows interacted.

Table 2 Characteristics of swirl configurations

Swirl configuration	45/50 deg	30/50 deg	30/−50 deg
Inner annulus vane angle	45 deg	30 deg	30 deg
Outer annulus vane angle	50 deg	50 deg	−50 deg
Swirl condition	Coswirl	Coswirl	Counterswirl

Initially, volumetric airflow rates of 14.3 SCFM were fed through each air annulus of the burner. This will be referred to as a 50/50% airflow distribution, where the first and second percentages indicate the proportion of the total air fed through the inner and outer annuli, respectively. All three swirl configurations were initially examined using this airflow distribution. Further experiments were carried out on the 30/−50 deg swirl configuration to determine the effect of airflow distribution using 25/75% and 60/40% airflow distribution in the burner.

Particle image velocimetry was used to examine the flow and recirculation regions associated with each swirl configuration under conditions of equal airflows (14.3 SCFM) in each annuli of the burner (i.e., 50/50% airflow distribution). The recirculation regions were examined under airflow-only conditions; the fuel spray was not present during this phase of the experiment. The presence of the fuel spray makes it difficult, if not impossible, to observe the motion of seed particles in the combustion air [27]. The inner and outer airstreams were seeded with latex microballoons, and the flow was illuminated with a vertical laser sheet from a twin-cavity Nd:YAG laser system. The mean diameter of the microballoons was approximately 5 μm. The laser sheet was projected though the vertical central cross section of the flow. Data on the flowfield characteristics were obtained at elevations between 8 and 45 mm downstream of the burner exit, and 39 mm on either side of the burner centerline. The PIV technique allowed the measurement of three components of velocity, but only the mean axial velocity is presented here, because the recirculation region is of primary interest in the analysis of swirl-stabilized flames. Mean velocities were obtained on the basis of 249 image pairs. Details of the PIV system used are given in Gupta et al. [21].

Design of the Fuel Pulsation System

To introduce modulated pulsations into the fuel flow, all fuel to the burner was routed through a solenoid-operated automotive fuel injector, designed to respond to a threshold voltage of 3 V. Figure 3 shows a schematic of the fuel delivery system. The fuel injector was installed in the fuel line upstream of the burner, and, when closed, interrupted the flow of fuel to the atomizing nozzle. When the necessary voltage was supplied, the solenoid valve in the injector opened; when this voltage was absent, the valve closed, and halted the flow of fuel through the supply line. To control the action of the valve, a signal generator was used to send a control voltage in the milliamp range to a solid-state amplifier. The amplifier then sent an amplified signal to the valve. The system, including the solenoid valve, was able to respond to signal frequencies between 0–1000 Hz. The shape of the solenoid valve flow curve could also be controlled by manipulating the voltage offsets of the control voltage; thus, in a given cycle, the solenoid valve could be open for varying periods of time. It was found that the flame responded best when the solenoid valve was open for 22% of a given cycle. If the solenoid valve was

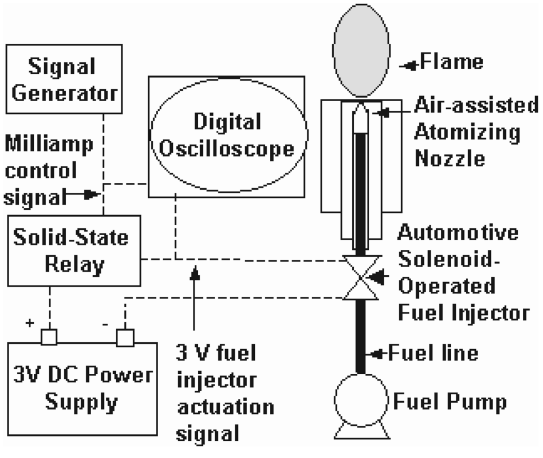

Fig. 3 Schematic diagram of the spray burner fuel delivery system.

open for too large a portion of the cycle, the fuel line downstream of the solenoid valve damped out the oscillation, and no cyclical instabilities in the flame were observed. If the solenoid valve was open for too small a period during the cycle, the mean fuel flow rate dropped dramatically, requiring high fuel pressures upstream of the solenoid valve to maintain a mean fuel flow rate of 0.5 gal/h.

To obtain good data, it was necessary to bleed the entire fuel system. The mean fuel flow rate was adjusted manually, upstream of the solenoid valve. When the solenoid valve was cycled at a given frequency, the upstream fuel pressure was adjusted to maintain a constant mean fuel flow rate. Thus, the introduction of pulsation into the fuel flow rate was the only change in the conditions examined for each pulsation frequency in a given swirl configuration.

The sound spectrum was obtained for each set of swirl and pulsation conditions using a sound spectrum analyzer capable of performing a fast Fourier transform on the frequency signals transmitted by a microphone. The microphone was a piezoelectric detector located 241 mm from the combustor vertical centerline, and 50 mm downstream of the burner exit.

Results and Discussion

Global Flame Features Without Fuel Pulsation

Flames observed with each of the three swirl configurations, with a 50/50% airflow distribution, and a steady fuel flow rate of 0.5 gal/h, are shown in Fig. 4. The 45/50 deg configuration has the greatest inner swirl angle; this produces the broadest and longest flame. The size and shape of the flame are directly linked to the features of the recirculation region associated with this swirl configuration. The flames produced with the 30/50 deg and 30/ − 50 deg flames are more compact, because they are stabilized by smaller, narrower recirculation regions. The 30/ − 50 deg flame appears to be larger than the 30/50 deg swirl configuration, and the flame front on the surface of the recirculation region extends farther upstream toward the fuel nozzle. This is attributed to more effective mixing in the counterswirling air case. The recirculation regions examined via PIV in the airflow associated with each flame are now discussed.

Characterization of Recirculation Region

The airflow field associated with each set of operating conditions has a dramatic effect on flame behavior. The inlet swirl strength and swirl distribution associated with the flow is an important parameter, particularly when a recirculation region is formed. Combustion occurs at the interface between the recirculation region and the surrounding flow, where hot recirculating gases and vaporized fuel come in contact with the oxidizer in the swirling combustion airstreams. The features of the flame are closely related to the features of the recirculation region, and direct characterization of this recirculation region is essential to analyze the swirl-stabilized flame structure and dynamic behavior.

Figures 5–7 show mean axial velocity contours associated with the 45/50 deg, 30/50 deg, and 30/ − 50 deg swirl configurations. The color scale in each figure relates the colors associated with each contour to the local axial mean velocity. All three figures show recirculation regions located downstream of the nozzle exit, over the burner centerline. In each figure, the origin of the coordinate system marks the fuel nozzle location.

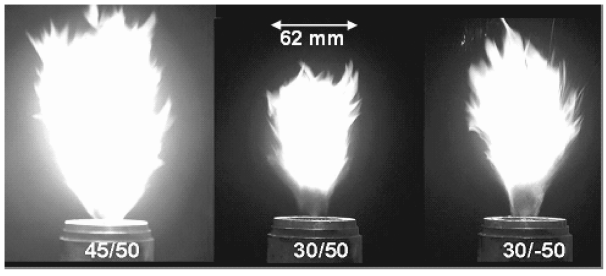

Fig. 4 Flames generated by 45/50 deg, 30/50 deg, and 30/ − 50 deg swirl combinations; 50/50% airflow distribution, 28.6 SCFM total airflow rate.

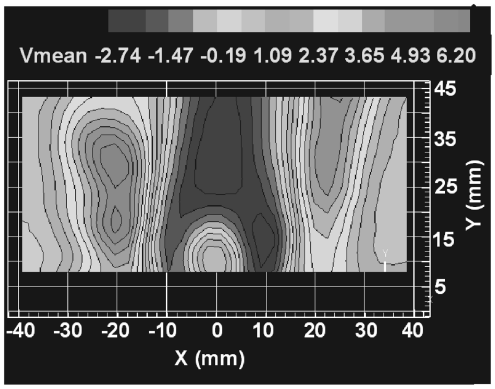

Fig. 5 Mean axial velocity contours (Vmean in m/s), 45/50 deg swirl configuration, 50/50% airflow distribution, 28.6 SCFM total airflow rate.

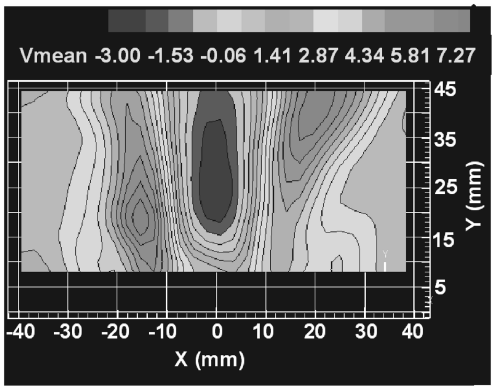

Fig. 6 Mean axial velocity contours (Vmean in m/s), 30/50 deg swirl configuration, 50/50% airflow distribution, 28.6 SCFM total airflow rate.

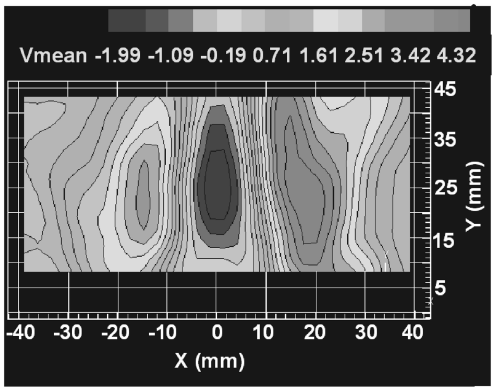

Fig. 7 Mean axial velocity contours (Vmean in m/s), 30/ − 50 deg swirl configuration, 50/50% airflow distribution, 28.6 SCFM total airflow rate.

The recirculation region associated with the 45/50 deg swirl configuration, shown in Fig. 5, is the largest of the three. This is to be expected, because this swirl configuration features the largest swirl number in the inner airflow. Negative axial velocities of up to −2.7 m/s are observed, and the recirculation region extends approximately 15 mm to either side of the burner centerline. The length of the recirculation zone extends upward in the axial direction beyond the examined region. This swirl configuration also produced the largest flame, as seen in Fig. 4.

Positive axial velocities, on the order of 2.3 m/s, are observed at the base of the recirculation region. These positive velocities are due

to the effect of atomization air, which emanates from the atomizing nozzle. The atomization air jet opposes recirculation and forces the recirculation region away from the fuel nozzle. As a result, the region is pushed downstream. This creates the slender base of the flames, just above the fuel nozzle, see Fig. 4.

Figure 6 shows mean axial velocity contours associated with the 30/50 deg swirl configuration. Because the swirl strength associated with this flow is smaller, the recirculation zone is smaller, and does not extend as far upstream or to either side of the burner centerline. The effect of the atomization air can be clearly observed; positive axial velocities are seen near the origin in Fig. 6, and the recirculation region is prevented from extending upstream to the fuel nozzle. In the positive axial direction, this recirculation zone also extends beyond the measurement region. Maximum negative mean axial velocities of -3.0 m/s are seen in the center of the recirculation zone.

The axial velocity contours obtained for the $30/-50$ deg configuration are shown in Fig. 7. The recirculation zone in this case resembles that seen in Fig. 6. This is not surprising, because the 30/50 deg and $30/-50$ deg swirl configurations share the same inner swirl vane angle and combustion airflow rates. Because the inner airstream has a larger velocity than the outer airflow, and an equal mass flow rate, the features of the air flowfield are most heavily affected by this inner air swirl in the combustor. However, Fig. 7 shows a more compact recirculation region than Fig. 6, and this is due to the effect of counterswirl. The counterswirling outer airstream present in the $30/-50$ deg configuration has the effect of opposing the rotation of the inner airstream somewhat, and converting rotational swirling motion into turbulence. Increased turbulence aids mixing at the boundary of the recirculation region and at the interface of two fluids [3]. However, it also effectively decreases the extent of the recirculation region, and this affects flame stability. Maximum negative mean axial velocities of -2.0 m/s are observed in this recirculation zone. The smaller recirculation velocities are due to the counterswirl condition.

It is also apparent that the luminous combustion zone associated with the counterswirling $30/-50$ deg flame in Fig. 4 is larger than that for the coswirling 30/50 deg case. This effect is also due to the degree of turbulent mixing associated with the counterswirl configuration, which distorts the flame front more extensively in the counterswirling flow and creates a larger region of luminosity [3]. The effects of co- and counterswirl on the flame dynamic response to forcing will now be presented.

System Response as a Function of Forcing Frequency

To examine flame response to an unstable equivalence ratio, the sound spectra of the flames were obtained. The 50/50% airflow distribution was employed. Background sound spectra with only the combustion airflow present were examined first. The sound spectra thus represented the background noise due to airflow through the ducts of the burner, blower motors, etc. The background noise, in the absence of a flame, must be characterized, so that it can later be removed from the sound spectrum associated with the combustor when a flame is present. The background spectra are shown in Fig. 8. The sound spectrum between 10 and 332 Hz is shown in Fig. 8a. A detailed view of the spectrum between 10 and 50 Hz is shown in Fig. 8b.

As can be seen from the figure, the swirl configuration had little effect on the background noise spectrum of the burner. All three swirl configurations display very similar background sound spectra. The important frequencies of the spectrum (such as the peak at 11 Hz) are determined by large components of the burner (such as the air ducts) and by features of the airflow, rather than by the particular swirl configuration.

For purposes of comparison, a baseline noise spectrum, with a steady fuel flow rate, then had to be established for each flame. These spectra, obtained under conditions where the solenoid valve remained open to provide a steady, uninterrupted fuel flow to the flame, are shown in Fig. 9. The background sound pressure levels, shown in Fig. 8, associated with each frequency in the spectrum have

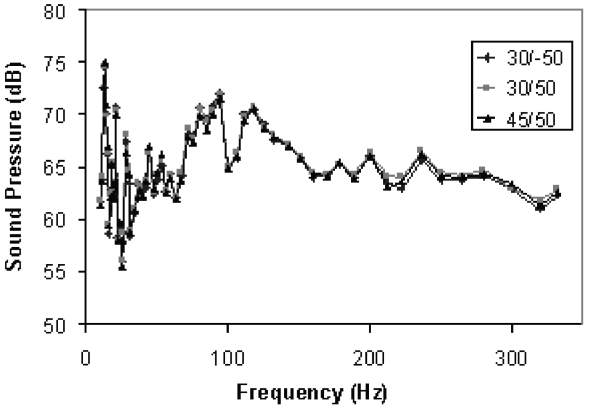

a) Frequency range 10-332 Hz

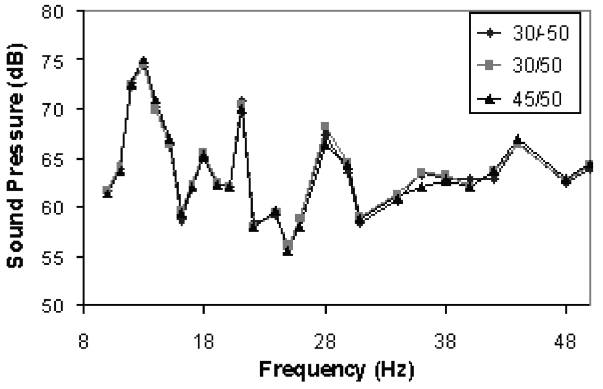

b) Frequency range 10-50 Hz

Fig. 8 Background noise spectra without fuel spray or flame.

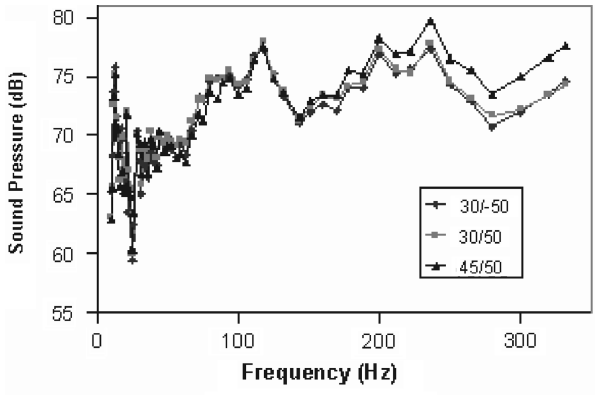

a) Frequency range 10-332 Hz

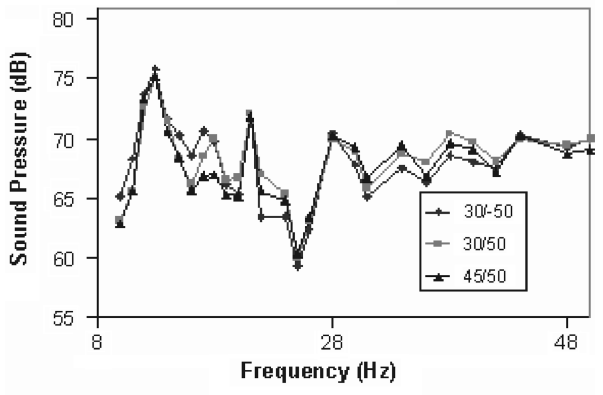

b) Frequency range 10-50 Hz

Fig. 9 Sound spectra of unforced flames.

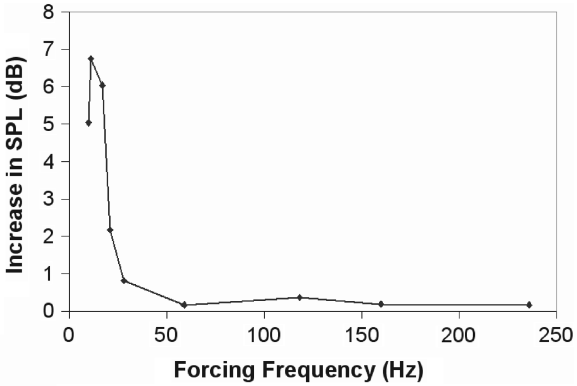

Fig. 10 Response of 45/50 deg flame at forced frequency to fuel pulsations.

been subtracted from the spectra shown in Fig. 9. The presence of a flame increases the sound pressure levels in the entire sound spectrum. This is not surprising, because the energy released by the dynamic expansion of gas from combustion causes increased sound pressure levels throughout the examined spectra. The most dramatic increases in sound pressure levels are seen at the higher frequencies, above 100 Hz, where the flame spectra display sound pressure levels up to 10 dB higher than the background spectrum. The sound pressure levels of frequencies above 100 Hz are approximately 2 dB higher for the 45/50 deg configuration than for the 30/50 deg and 30/−50 deg flames.

To assess the impact of the fuel pulsations at a particular frequency, the 45/50 deg swirl configuration in the combustor was forced at a number of frequencies corresponding to peaks seen in the sound spectrum for the unforced flame. These peaks indicate unstable modes of the flame, marking frequencies at which important turbulent events participate in combustion. The objective was to force these modes in such a way that they dominated the sound spectrum. Figure 10 shows the difference in sound spectrum intensity due to forcing at the forced frequency, measured in dB.

The increase in the sound pressure level was found to be most dramatic for frequencies in the lower range of the spectrum. For example, when the flame was forced at a frequency of 11 Hz, the flame displayed an increase in the sound pressure level of 6.75 dB at this frequency. This suggested that, to examine the impact of swirl configuration, it would be necessary to force at one of these lower frequencies. Further, it was noted that harmonics of the forced frequency would also show an elevated sound pressure when the fuel flow was modulated, but that this response was weak.

Based on the behavior of the 45/50 deg swirl configuration, it was decided to force the flame at 15 Hz. When the pulsation signal at 15 Hz was introduced into the combustor, the flame characteristics were observed to change considerably for each flame. A strobing effect, in sync with the fuel pulsation, was observed, and the brightness and size of the flames cycled in time with the pulsation, indicating a fluctuation in the flame heat release. The change in sound of the flames was audible; a low-frequency rumble dominated the tone produced by each flame when the fuel pulsation was introduced.

The resulting flame sound spectra, obtained for each swirl configuration when the combustor was forced at 15 Hz are shown in Fig. 11. The sound spectrum from 10 to 332 Hz is displayed in Fig. 11a while the sound spectrum between 10 and 50 Hz is shown in Fig. 11b. Each forced spectrum shows a dramatic increase in sound pressure level at the forcing frequency of 15 Hz. Higher harmonics of the forcing frequency also show an increase in amplitude, resulting in peaks at 31 and 44 Hz. The most dramatic response is seen from the 30/−50 deg flame, which displays a peak sound pressure level of 92.2 dB at 15 Hz. This is a significant increase in sound pressure level; when no forcing was present, the 30/−50 deg flame displayed a sound pressure level of only 70.3 dB at 15 Hz. The increase in sound pressure level at the forcing frequency and at the first and second harmonics of the forcing frequency for each swirl combination is shown in Fig. 12.

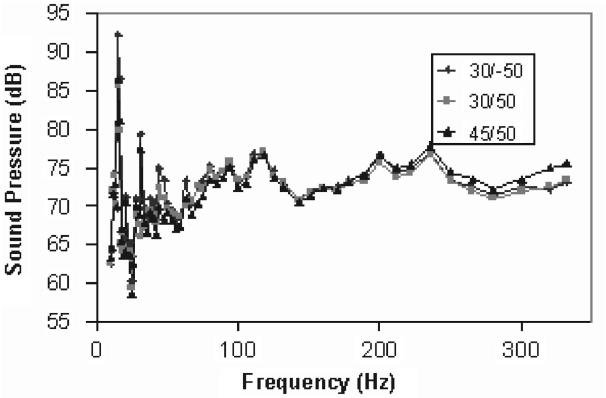

a) Frequency range 10-332 Hz

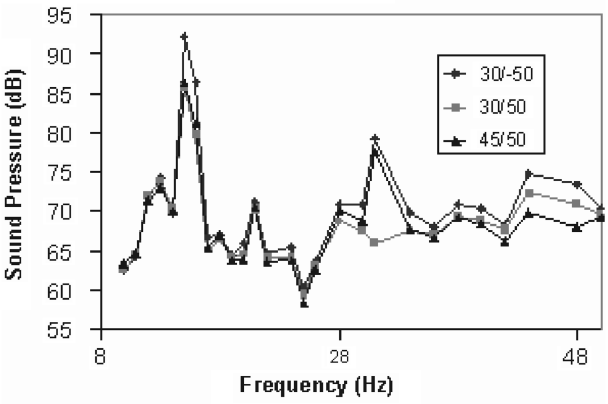

b) Frequency range 10-50 Hz

Fig. 11 Sound spectra of forced flames with input signal at 15 Hz.

Figure 12 shows that swirl configuration has an impact on the response of the flame to the introduction of instability in the fuel flow. The 30/−50 deg configuration displayed a significant increase in sound pressure level at 15, 31, and 44 Hz. The 30/50 deg configuration displayed a less pronounced increase in amplitude at the forcing frequency (15 Hz), no significant response at 30 Hz, and a moderate increase of 2.5 dB in the amplitude at the 44 Hz signal. The 45/50 deg configuration displayed a response close to that of the 30/−50 deg configuration at 15 and 30 Hz, but no increase whatsoever in amplitude in the 44 Hz signal. In fact, a slight decrease of 0.1 dB was observed.

It is important to note that the sound pressure spectrum is not the only characteristic of the flames that is affected by fuel pulsation. Combustion completeness, flame chemistry, and fuel atomization are all affected by the fuel flow behavior. What does appear to be significant is the difference in dynamic response observed for each swirl configuration. These flames responded quite differently to the same input signal, indicating that passive control techniques based

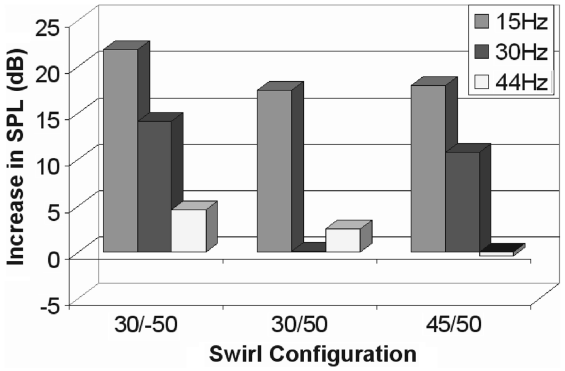

Fig. 12 Flame acoustic response to forcing at 15 Hz with response shown at forcing frequency and harmonics.

on swirl distribution can have a significant impact on controlling instabilities in spray flames.

Observation of Dynamic Flame Structure

To examine the physics of the flame instability produced by the forcing signal, a CCD camera was used to record the global structure of the unstable flames at 30 Hz from the three swirl configurations. The global structure images were then examined to track the development of the luminous region of the flame during the instability cycle. Because the heat-release signature of kerosene flames is closely linked to the flame luminosity, it is possible to examine the evolution of the heat-release characteristics of the flame during the cycle of the instability. The structure of the luminous region, where heat release occurs, can be observed near the peak and minimum of the heat-release cycle. The differences between the three flames are most dramatic at these points during the cycle.

The structure of the 45/50 deg flame near peak and minimum heat release is shown in Fig. 13. Near peak heat release (shown on the left in Fig. 13), the flame is a tall column with the luminous flame region extending more than 3.8 burner diameters downstream. When the heat release is near its minimum (shown on the right in Fig. 13), the flame region is much smaller, and extends only 2.9 burner diameters downstream. The flame region is detached from the burner during this phase. Fuel concentrations near the nozzle decrease, and combustion is sustained by unburned fuel entrained in the recirculation region. This explains why the 45/50 deg flame did not respond readily to forcing at higher frequencies (see Fig. 10), and why the highest harmonic of the forcing frequency (at 44 Hz) could not be excited (see Fig. 12). The effect of any interruption in the fuel flow, or change in the spray characteristics, at higher forcing frequencies is damped out by the stabilizing effect of the large volume of entrained gases in the recirculation zone. However, at low forcing frequencies, the large volume of recirculating gas effectively heats and ignites the fuel spray burst occurring during the peak heat-release phase of the cycle.

For the 30/50 deg swirl configuration, the flame structure near peak heat release is different than for the 45/50 deg swirl case. Instead of forming a tall column, the flame is confined to a brush-shaped region (shown on the left in Fig. 14), formed when a cloud of fuel is ejected from the fuel nozzle. In this flame, the recirculation region is much smaller; as a result, the volume of unburned fuel available to sustain the flame through the minimum heat-release phase of the cycle is smaller. This phase is shown on the right in Fig. 14. As can be seen, the flame region above the nozzle decreases dramatically in size. The combustion is confined to a small region, less than a burner diameter in length, positioned immediately over

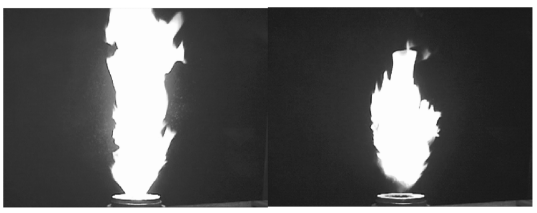

Fig. 13 Images of forced 45/50 deg flame. Left image: Flame near peak heat release. Right image: Flame near minimum heat release.

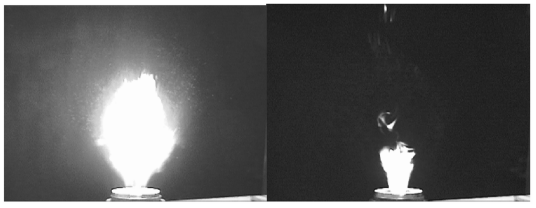

Fig. 14 Images of 30/50 deg coswirling flame. Left image: Flame near peak heat release. Right image: Flame near minimum heat release.

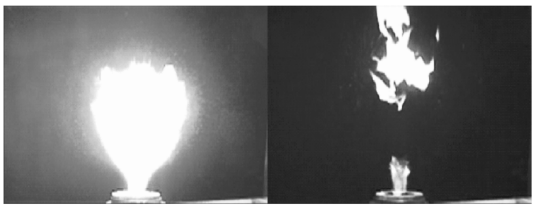

Fig. 15 Images of 30/ − 50 deg counterswirl flame. Left image: Flame near peak heat release. Right image: Flame near minimum heat release.

the atomizing nozzle during the minimum heat-release phase of the cycle.

This effect is even more dramatic for the 30/ − 50 deg swirl configuration. As can be seen on the left and right sides of Fig. 15, the flame structure cycles even more dramatically when this swirl configuration is used. During the peak heat-release phase of the cycle (shown on the left), the flame brush resembles that seen from the 30/50 deg swirl configuration; however, during the minimum phase of the cycle, the flame is reduced to a small blue flame directly above the fuel nozzle (shown on the right). Because of the counterswirl configuration, the recirculation region is weakened somewhat; and increased mixing due to the counterswirling airflow in the region above the burner dilutes any hot gases present with cooler air. Hot product gases are not recirculated effectively, in a way that would allow the instability to be damped. However, when fresh fuel exits the nozzle during the next period of maximum heat release, it mixes rapidly with combustion air due to the counterswirling flow, it is rapidly ignited by the remaining flame at the nozzle, and burns out rapidly. The resulting combustion gases are then diluted and convected downstream; this effect is also evidenced by the flamelets entrained in the airflow above the nozzle in the image on the right side of Fig. 15. This combination of effects appears to account for the sensitivity of this flame to instabilities in the fuel flow.

Effect of Airflow Distribution

The effect of airflow distribution on the unstable response of the flame is now examined. The 30/ − 50 deg swirl configuration was selected for further examination, because its unstable response to forcing was larger than those associated with the other two swirl configurations. The total amount of air fed to the burner was constant, remaining at 28.6 SCFM. However, the proportion of air fed through the inner and outer air ducts was varied, so that the proportion of the total air fed through each duct was changed. In the 25/75% distribution, 25% of the total air, or 7.15 SCFM, was fed through the inner air annulus, and 21.45 SCFM of air, or 75% of the total air, was fed through the outer annulus. The behavior of the 30/ − 50 deg flame with a 50/50% airflow distribution has already been described above. In addition, a 60/40% distribution was also examined.

The flames obtained from the 30/ − 50 deg swirl configuration with the three airflow distributions were all found to respond to forcing. The response of the sound pressure levels at the forcing frequency and higher harmonics is shown in Fig. 16. As can be seen from the figure, an increase in the proportion of air fed through the inner annulus increases the unstable response of the flame. The sound pressure level of every frequency examined, including the first and second harmonics, increased by several decibels. There was a 7.1 dB increase in the sound pressure level at 15 Hz when the proportion of air fed through the inner annulus was increased from 25 to 50%.

The reason appears to be related to the extent of the recirculation region in the flow. The relatively weak swirl imparted to the air emerging from the inner annulus did not form a broad or extensive recirculation region. Because the airflow fed through the outer annulus had a higher level of swirl in this configuration, increasing the proportion of air fed through the outer annulus spread the flow radially, thus decreasing the axial velocity. The outer air annulus also had a larger cross-sectional area at the outlet; thus, if the same mass flow rate was fed through the larger duct, the total velocity of the flow decreased. Hot gases and combusting gases thus had a much longer residence time, and the unstable response of the burner to oscillatory

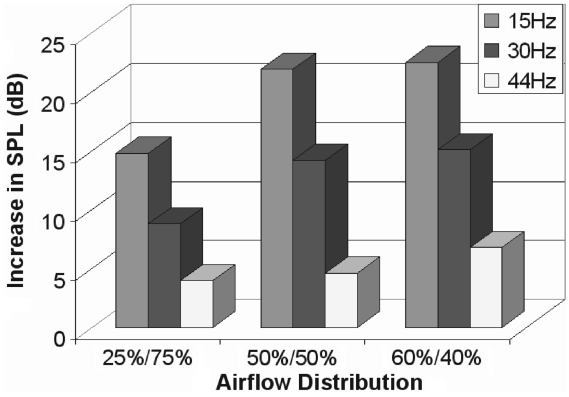

Fig. 16 Effect of airflow distribution on flame acoustic response to forcing at 15 Hz with response shown at forcing frequency and higher harmonics.

equivalence ratio was far less severe. The rate of heat release remained more stable during the fuel-lean, minimum heat-release phase of the instability cycle, since combusting gases were convected out of the reaction region more slowly. The flame then reignited less abruptly when the fuel spray was reintroduced during the fuel-rich phase, because some quantities of unburned fuel were still present from the previous cycle, and the mechanisms of turbulent mixing leading to ignition occurred more slowly when the airflow velocities were lower.

Summary

Passive control of swirling spray flames has been demonstrated using radial distribution of swirl and airflow to a coannular, swirl-stabilized spray burner. The installation of a solenoid valve in the fuel line, along with the necessary signal generator and amplification electronics, has made it possible to introduce oscillations in the equivalence ratio of the flame. The effects of co- and counterswirl airflows and airflow distribution in the burner on the structure and dynamic response of the flame have been examined.

The structures of unforced flames, obtained with a steady fuel flow rate were found to depend heavily on the features of the recirculation region associated with the combustion airflow. The recirculation regions in the nonreacting airflow associated with each case were examined directly using PIV diagnostics. An increase in the swirl number associated with inner annulus airflow was found to increase the size of the recirculation region, thus creating a larger flame. A counterswirling swirl condition was found to produce an increase in turbulent distortion of the flame.

The effect of swirl configuration and airflow distribution on the dynamic response of the spray flames to an oscillatory equivalence ratio has been investigated. When low-frequency instabilities were introduced into the fuel flow, the response of the flame was found to depend to a great extent on the swirl configuration. Larger recirculation regions in the flow and airflow distributions that increase the residence time of product gases and combusting gases above the burner improved flame stability. The $30/-50$ deg configuration responded most dramatically, displaying an increase in the sound pressure level at the forced frequency of over 20 dB when equal flow rates of air were fed through the inner and outer air annuli. Higher harmonics of the forced frequency were also readily excited for this swirl configuration. The response of the 30/50 deg and 45/50 deg configurations were less dramatic. The 30/50 deg flame showed the smallest increase in sound pressure level at the forcing frequency, and also damped out the higher harmonics of the forced frequency. This flame may have had a smaller acoustic response than either the 45/50 deg or $30/-50$ deg flame for reasons related to completeness of combustion. This flame featured neither the extensive recirculation region of the 45/50 deg flame, nor the aggressive mixing associated with the counterswirl configuration; it is likely that some of the fuel was simply not burned effectively. The total heat release of the flame is thus lower, and thus less energy was available to drive unstable behavior.

Passive control of combustion driven instability can be obtained using radial distribution of swirl and changing the airflow distribution in the burner. On the basis of the above findings, it is to be expected that spray flames featuring large recirculation regions will be less vulnerable to high-frequency instabilities, and that spray flames whose airflow fields are configured to achieve the longest residence times will be generally less susceptible to instabilities in the fuel flow rate. These observations demonstrate the practical applicability of swirl and flow distribution as a means of passive control.

Acknowledgment

The support of the Office of Naval Research, program manager Gabriel D. Roy is gratefully acknowledged.

References

[1] Sivasegaram, S., and Whitelaw, J. H., "Suppression of Oscillations in Confined Disk-Stabilized Flames, "*Journal of Propulsion and Power*, Vol. 3, No. 4, 1987, pp. 291–295.

[2] Rayleigh, J. W. S., *The Theory of Sound*, Vol. 2, Dover Publications, New York, 1945, pp. 170–235.

[3] Gaydon, A. G., and Wolfhard, H. G., *Flames, Their Structure, Radiation, and Temperature*, Wiley, New York, 1979.

[4] Schadow, K. C., and Gutmark, E., "Combustion Instability Related to Vortex Shedding in Dump Combustors and Their Passive Control," *Progress in Energy and Combustion Science*, Vol. 18, No. 2, 1992, pp. 117–131.

[5] Gutmark, E. J., and Grinstein, F. F., "Flow Control with Noncircular Jets," *Annual Review of Fluid Mechanics*, Vol. 31, Jan. 1999, pp. 239–272.

[6] Schadow, K. C., Gutmark, E., Wilson, K. J., and Smith, R. A., "Multistep Dump Combustor Design to Reduce Combustion Instabilities," *Journal of Propulsion and Power*, Vol. 6, No. 4, 1990, pp. 407–411.

[7] Paschereit, C. O., and Gutmark, E., "Passive Combustion Control Applied to Premix Burners," AIAA Paper 2002-1007, Jan. 2002.

[8] Hu, H., Saga, T., Kobayashi, T., and Taniguchi, N., "Passive Control on Jet Mixing Flows by Using Vortex Generators," *6th Triennial Symposium on Fluid Control*, Aug. 2000.

[9] Steele, R. C., Cowell, L. K., Cannon, S. M., and Smith, C. E., "Passive Control of Combustion Instability in Lean Premixed Combustors," *Journal of Engineering for Gas Turbines and Power*, Vol. 122, No. 3, July 2000, pp. 412–419.

[10] Smith, C. D., and Cannon, S. M., "CFD Assessment for Passive and Active Control Strategies for Lean, Premixed Combustors," AIAA Paper 99-0714, Jan. 1999.

[11] Richards, G. A., and Janus, M. C., "Characterization of Oscillations During Premix Gas Turbine Combustion," ASME Paper 97-GT-244, June 1997.

[12] Nasr, G. G., Yule, A. J., and Bendig, L., *Industrial Sprays and Atomization: Design, Analysis and Applications*, Springer, London, 2002.

[13] Lubarsky, E., and Levy, Y., "Experimental Investigation of Flame-Holding System for the Suppression of Ramjet Rumble," *Proceedings of the 27th Symposium (International), on Combustion*, The Combustion Institute, Boulder, CO, Aug. 1998, pp. 2033–2037.

[14] Gupta, A. K., Lilley, D. G., and Syred, N., *Swirl Flows*, Abacus Press, Tunbridge Wells, U.K., 1984.

[15] Mehresh, P., Habibzadeh, B., and Gupta, A. K., "Control of Spray Flame Characteristics Using High Shear in a Double Concentric Swirl Burner," *Proceedings of the 2002 International Joint Power Generation Conference (IJPGC)*, American Society of Mechanical Engineers, Fairfield, NJ, June 2002, pp. 1027–1037.

[16] Gao, Z., Mashayek, F., Linck, M., and Gupta, A. K., "Experimental Results and Calculations of 2-Phase Flow in a Swirl Burner Under Isothermal Condition," AIAA Paper 2003-0336, Jan. 2003.

[17] Linck, M., Armani, M., and Gupta, A. K., "Flow Characteristic Effects on Exhaust Gas Composition in Kerosene Spray Flames," AIAA Paper 2003-5929, Aug. 2003.

[18] Linck, M., Armani, M., and Gupta, A. K., "Passive Control of Unstable Combustion in a Swirl-Stabilized Spray Combustor," AIAA Paper 2004-0810, Jan. 2004.

[19] Linck, M., Armani, M., and Gupta, A. K., "Effect of Swirl and Fuel Pulsation on Flame Dynamics, Flame Structure, and Droplet Dynamics in Swirl Stabilized Spray Flames," PWR Paper 2004-52048,

March 2004.
[20] Gupta, A. K., and Linck, M., "Passive Control of Flow and Flame Structure in Spray Combustion," *International Colloquium on Combustion Control*, Cranfield University, Cranfield, U.K., Aug. 2003.
[21] Gupta, A. K., Lourenco, L., Linck, M., and Archer, S., "A New Method to Measure Flowfield in Luminous Spray Flames," *Journal of Propulsion and Power*, Vol. 20, No. 2, March–April 2004, pp. 369–372.
[22] Linck, M., and Gupta, A. K., "Effect of Swirl and Combustion on Flow Dynamics in Luminous Kerosene Spray Flames," AIAA Paper 2003-1345, Jan. 2003.
[23] Conrad, T. J., Bibik, A., Lee, J. Y., Shcherbik, D., Lubarsky, E., and Zinn, B. T., "Control of Combustion Instabilities by Fuel Spray Modification Using Smart Fuel Injector," AIAA Paper 2003-4937, July 2003.
[24] Timmler, J., and Roth, P., "Optical Measurement of Droplet Evaporation Rates," *Optical Particle Sizing: Theory and Practice*, Plenum Press, New York, 1988, pp. 511–522.
[25] Presser, C., Gupta, A. K., Avedisian, C. T., and Semerjian, H. G., "Effect of Dodecanol Content on the Combustion of Spray Flames," *Atomization and Sprays*, Vol. 4, No. 3, 1994, pp. 207–222.
[26] Bachalo, W. D., and Houser, M. J., "Phase/Doppler Spray Analyzer for Simultaneous Measurements of Drop Size and Velocity Distributions," *Optical Engineering*, Vol. 23, No. 5, 1984, pp. 583–590.
[27] Raffel, M., Willert., C., and Kompenhans, J., *Particle Image Velocimetry, A Practical Guide*, Springer–Verlag, Berlin, 1998.

C. Avedisian
Associate Editor